

Multi-color mechanochromic luminescence of three polymorphic crystals of a donor–acceptor-type benzothiadiazole derivative

Suguru Ito,^{*a} Sayaka Nagai,^a Takashi Ubukata^a and Takashi Tachikawa^b

*^aDepartment of Chemistry and Life Science, Graduate School of Engineering Science,
Yokohama National University*

79-5 Tokiwadai, Hodogaya-ku, Yokohama 240-8501, Japan

**E-mail: suguru-ito@ynu.ac.jp*

^bDepartment of Chemistry, Graduate School of Science, Kobe University,

1-1 Rokkodai-cho, Nada-ku, Kobe 657-8501, Japan

^cMolecular Photoscience Research Center, Kobe University,

1-1 Rokkodai-cho, Nada-ku, Kobe 657-8501, Japan

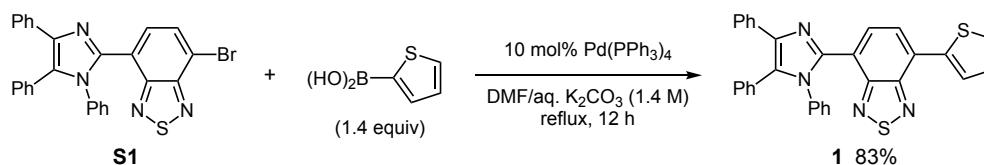
Table of contents

| | |
|---|-----|
| 1. Synthesis and single-crystal X-ray diffraction analyses..... | S2 |
| 2. Supplementary spectra for the mechanochromic luminescence..... | S4 |
| 3. DSC thermograms for the crystalline and amorphous samples..... | S5 |
| 4. Measurements of fluorescence lifetimes..... | S5 |
| 5. Theoretical calculations..... | S8 |
| 6. PXRD analysis..... | S9 |
| Reference..... | S9 |
| NMR spectra..... | S10 |

1. Synthesis and single-crystal X-ray diffraction analyses

Synthesis of 1

Thienyl-substituted derivative **1** was synthesized by the Suzuki–Miyaura coupling between 4-bromo-7-(1,4,5-triphenyl-1*H*-imidazol-2-yl)benzo[*c*][1,2,5]thiadiazole and 2-thienylboronic acid in 83% yield.



Scheme 1. Synthesis of thienyl-substituted donor–acceptor-type benzothiadiazole derivative **1**

X-ray structures of 1

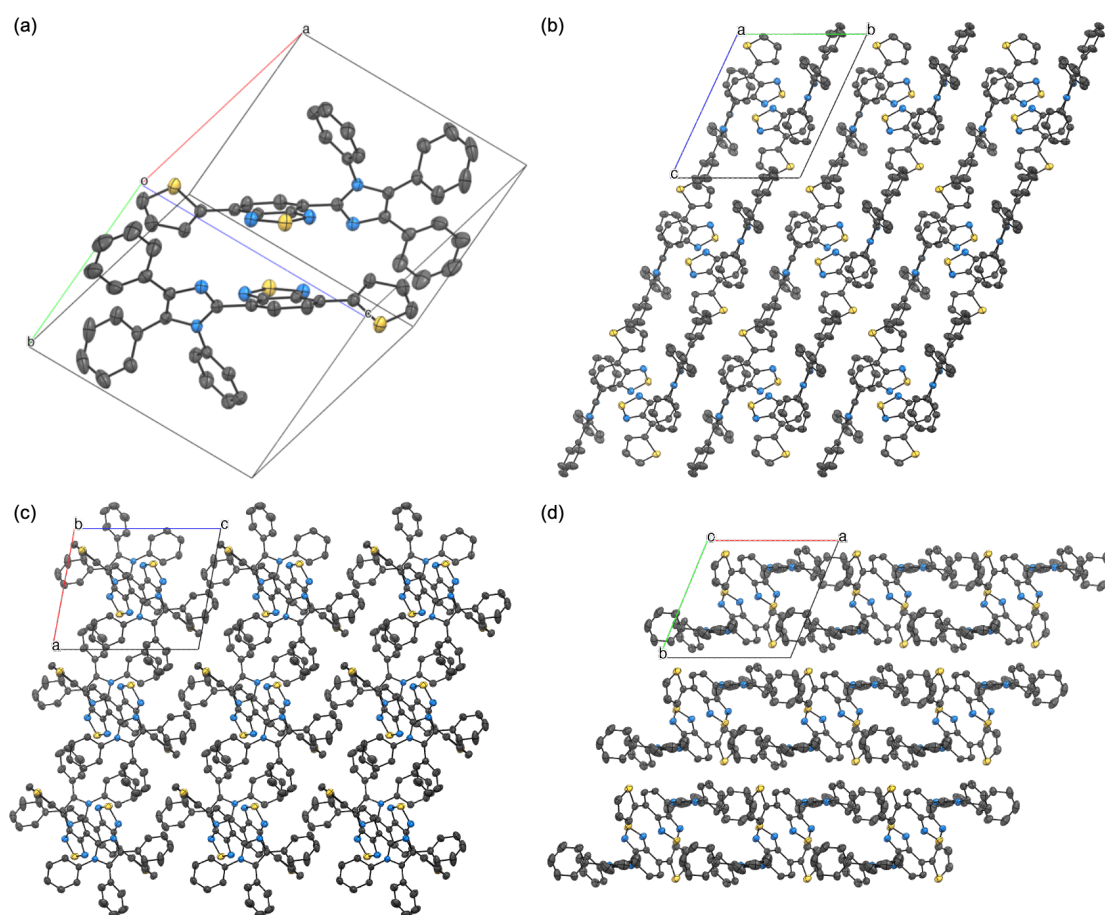


Fig. S1 The packing structure of **1- α** (CCDC 2073080) with atomic displacement parameters set at 50% probability (Color code: gray = C, blue = N, yellow = S). All hydrogen atoms are omitted for clarity. (a) Unit cell structure. (b) Viewed along *a*-axis. (c) Viewed along *b*-axis. (d) Viewed along *c*-axis.

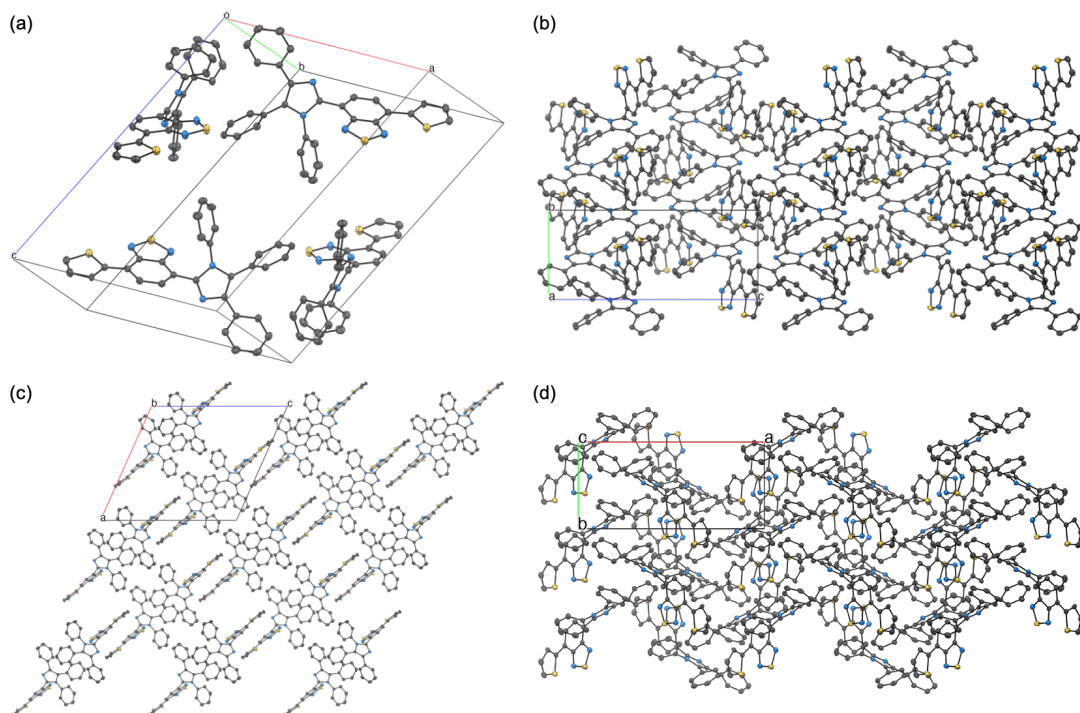


Fig. S2 The packing structure of **1-β** (CCDC 2073081) with atomic displacement parameters set at 50% probability (Color code: gray = C, blue = N, yellow = S). All hydrogen atoms are omitted for clarity. (a) Unit cell structure. (b) Viewed along *a*-axis. (c) Viewed along *b*-axis. (d) Viewed along *c*-axis.

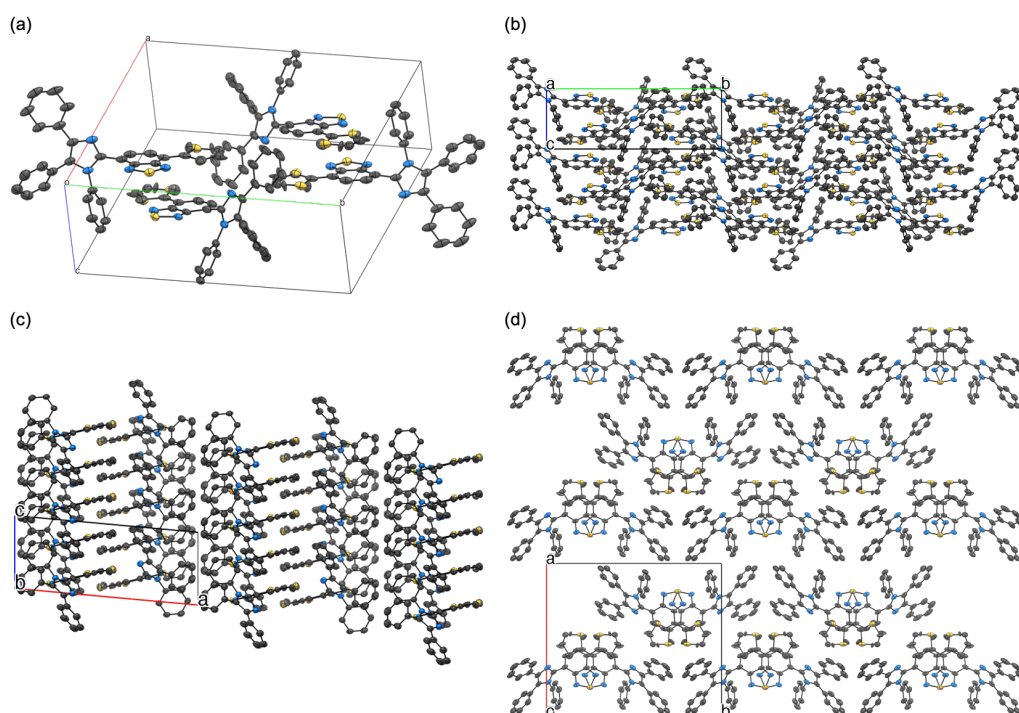


Fig. S3 The packing structure of **1-γ** (CCDC 2073082) with atomic displacement parameters set at 50% probability (Color code: gray = C, blue = N, yellow = S). All hydrogen atoms are omitted for clarity. (a) Unit cell structure. (b) Viewed along *a*-axis. (c) Viewed along *b*-axis. (d) Viewed along *c*-axis.

2. Supplementary spectra for the mechanochromic luminescence

Fluorescence spectra showed significant shifts in maximum emission wavelengths for the bicolor MCL of **1- α** and tricolor emission switching of **1- β** and **1- γ** (Fig. S4).

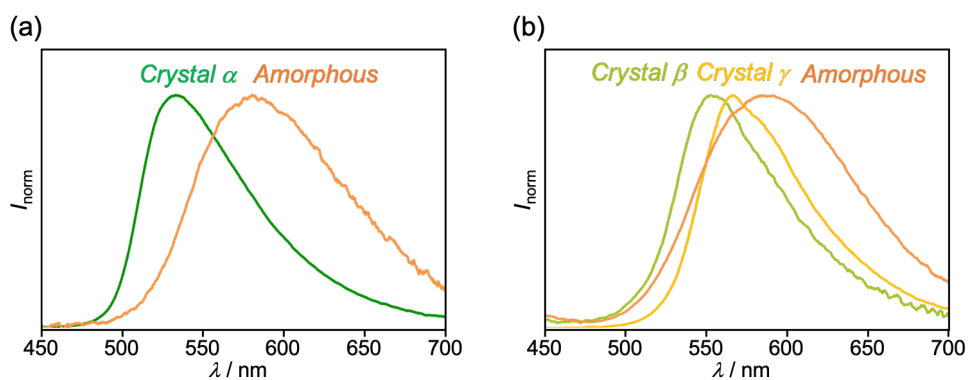


Fig. S4 Fluorescence spectra for (a) bicolor MCL of **1- α** and (b) tricolor emission switching of **1- β** and **1- γ** ($\lambda_{\text{ex}} = 365 \text{ nm}$).

In the samples where the emission wavelength was observed in the long-wavelength region, both the absorption and excitation spectra were observed in the long-wavelength region (Fig. S5). Therefore, changes in the molecular conformation and intermolecular interactions in the ground state should contribute to the difference in the emission wavelength of these samples.

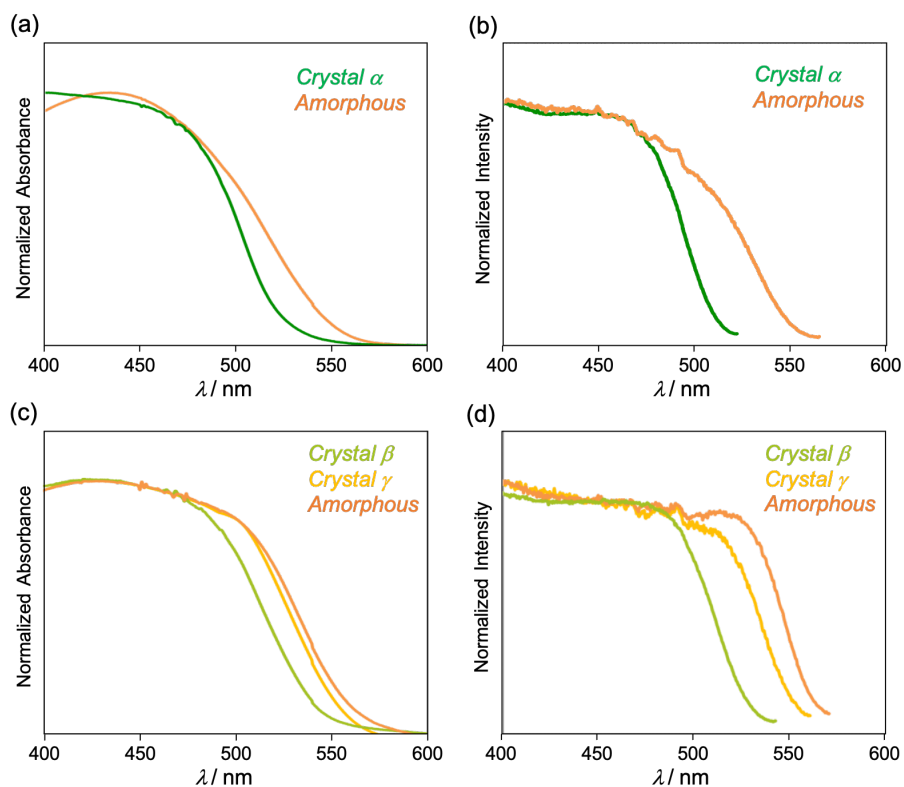


Fig. S5 Absorption (a and c) and excitation (b and d) spectra for bicolor MCL of **1- α** (a and b) and tricolor emission switching of **1- β** and **1- γ** (c and d).

3. DSC thermograms for the crystalline and amorphous samples

Comparing the enthalpy values of the melting point for crystalline **1- α** and the corresponding ground state, the ground sample showed a smaller value (Fig. S6). Although the crystallinity of **1- α** was restored by heating, the heated sample would contain a portion of the amorphous phase.

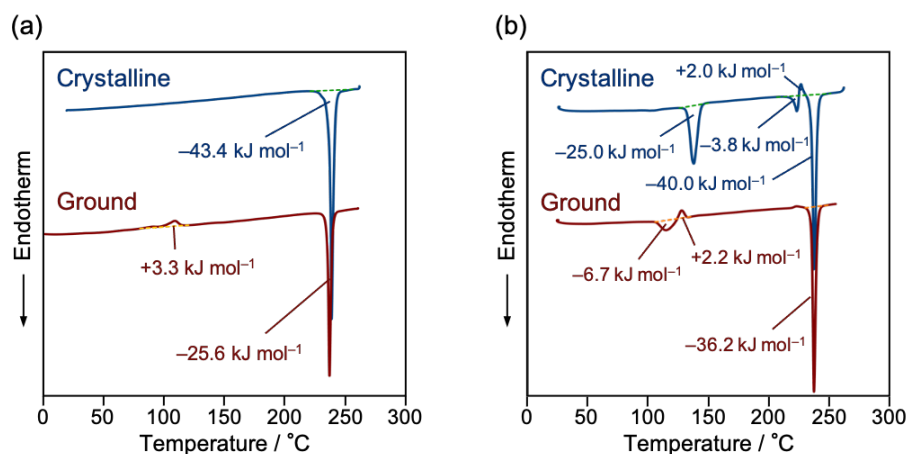


Fig. S6 DSC thermograms for the crystalline and ground samples of **1- α** (a) and **1- β** (b). Enthalpy values are noted near the corresponding peaks.

4. Measurements of fluorescence lifetimes

Measurements of fluorescence lifetimes were performed on a home-built wide-field/confocal microscope equipped with a Nikon Ti-E inverted fluorescence microscope. The fluorescence images were recorded using a color sCMOS camera (Dhyana 400DC, Tucson Photonics). The 405-nm continuous wave laser (OBIS 405LX, Coherent) or 405-nm pulsed diode laser (PiL040X, Advanced Laser Diode System, 45-ps FWHM) was used to excite the samples. A dichroic mirror (Di02-R405, Semrock) and a longpass filter (ET425lp, Chroma) were used to filter the scattering from excitation light. For the spectroscopy, only the emission that passed through a slit entered the imaging spectrograph (MS3504i, SOL instruments) equipped with a CCD camera (DU416A-LDC-DD, Andor). For time-resolved fluorescence measurements, the emitted photons were passed through a 100- μm pinhole and then directed onto a single-photon avalanche diode (SPD-050, Micro Photon Devices). The signals from the detector were sent to a time-correlated single photon counting module (SPC-130EM, Becker & Hickl) for further analysis. The instrument response function of the system was about 100 ps. All the experiments were conducted at room temperature. The data were analyzed using ImageJ (<http://rsb.info.nih.gov/ij/>) and Origin 2021 (OriginLab).

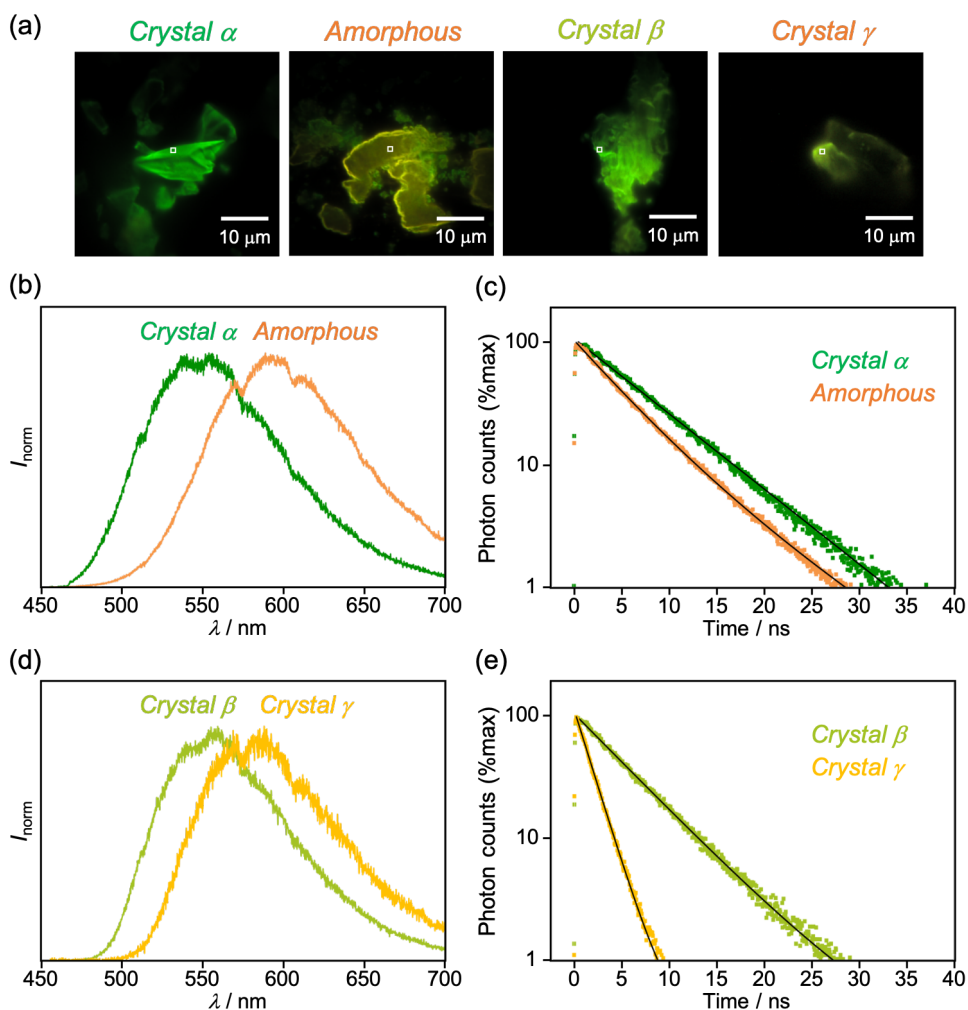


Fig. S7 Photographs, fluorescence spectra, and fluorescence decay profiles recorded at the single-particle level ($\lambda_{\text{ex}} = 405 \text{ nm}$). (a) Photographs of crystal **1- α** , ground amorphous sample of **1- α** , crystal **1- β** , and crystal **1- γ** . The square marks indicate the measured locations of fluorescence spectra and fluorescence decay profiles. (b) Fluorescence spectra of crystal **1- α** (green) and ground amorphous sample of **1- α** (orange). (c) Fluorescence decay profiles of crystal **1- α** (green) and ground amorphous sample of **1- α** (orange) monitored $>425 \text{ nm}$. The black lines indicate single- (crystal α) and double-exponential (amorphous) curves fitted to the time profiles. (d) Fluorescence spectra of crystal **1- β** (yellowish green) and **1- γ** (yellowish orange). (e) Fluorescence decay profiles of crystal **1- β** (yellowish green) and **1- γ** (yellowish orange) monitored $>425 \text{ nm}$. The black lines indicate double-exponential curves fitted to the time profiles.

The fluorescence decay profiles of crystalline and ground amorphous samples of **1- α** were fitted well to the single- and double-exponential functions ($R^2 > 0.998$). Crystal **1- β** and crystal **1- γ** were fitted well to the double-exponential functions ($R^2 > 0.998$), in which the contributions of minor components were trivial. The emission wavelength, intensity-weighted mean fluorescence lifetime ($\langle\tau\rangle$), fluorescence lifetime (τ_n), coefficient of determination (R^2), and radiative (k_r) and non-radiative rate constants (k_{nr}) of these samples are shown in Table S1.

Table S1. Emission wavelength, intensity-weighted mean fluorescence lifetime ($\langle\tau\rangle$), fluorescence lifetime (τ_n), coefficient of determination (R^2), and radiative (k_r) and non-radiative rate constants (k_{nr}) of polymorphic and amorphous samples of **1.^a**

| Sample | λ_{em} (nm) ^b | $\langle\tau\rangle$ (ns) ^c | τ_1 (ns) ^d | τ_2 (ns) ^d | R^2 | k_r (10^7 s^{-1}) ^e | k_{nr} (10^7 s^{-1}) ^e |
|------------------------------------|-------------------------------------|---|-------------------------------|-------------------------------|---------|---|--|
| Crystal α | 545 | 7.03 | 7.025 \pm 0.017 (1.00) | | 0.99802 | 8.5 | 5.7 |
| Amorphous | 590 | 5.96 | 4.554 \pm 0.127 (0.65) | 8.599 \pm 0.628 (0.35) | 0.99891 | 8.2 | 8.6 |
| Crystal β | 555 | 6.04 | 5.445 \pm 0.049 (0.96) | 19.77 \pm 9.63 (0.04) | 0.99853 | 5.5 | 11.1 |
| Crystal γ | 580 | 2.43 | 1.722 \pm 0.005 (0.95) | 16.17 \pm 2.97 (0.05) | 0.9992 | 4.5 | 36.6 |

^aExcitation wavelength for the measurement of the fluorescence lifetime is 405 nm. ^b Maximum emission wavelength observed by the fluorescence microscopy. ^c Intensity-weighted mean fluorescence lifetime $\langle\tau\rangle = f_1\tau_1 + f_2\tau_2$. ^d The fractional contribution f_n of the component is shown in parentheses. ^e k_r and k_{nr} were calculated from $\Phi_F = k_r/(k_r + k_{nr}) = \langle\tau\rangle \times k_r$.

5. Theoretical calculations

Experimental absorption maxima and the results of DFT and TD-DFT calculations are shown in Table S2. The HOMO and LUMO orbitals of dimer **1** in **1- α** , **1- β** , and **1- γ** are shown in Fig. S8.

Table S2 Experimental absorption maxima and calculated absorption properties.

| Crystal | Absorption in toluene λ_{abs} (nm) | Calcd absorption λ_{abs} (nm) | Transition from HOMO to LUMO | Oscillator strength | HOMO (eV) | LUMO (eV) | Dipole moment (D) |
|---|---|--|---------------------------------|------------------------|--------------|--------------|-------------------------|
| 1-α | 436 | 375.63 | 0.617 | 0.3287 | -6.60 | -1.28 | 3.73 |
| 1-α2^a | | 379.96 | 0.539 | 0.0000 | -6.56 | -1.20 | 0.01 |
| 1-β | 436 | 387.07 | 0.568 | 0.3783 | -6.54 | -1.35 | 3.78 |
| 1-β2^a | | 389.46 | 0.593 | 0.6463 | -6.44 | -1.18 | 0.00 |
| 1-γ | 436 | 397.77 | 0.621 | 0.3713 | -6.50 | -1.37 | 3.75 |
| 1-γ2^a | | 407.83 | 0.428 | 0.1594 | -6.38 | -1.39 | 7.38 |

^a The dimer molecules in spatial proximity were calculated

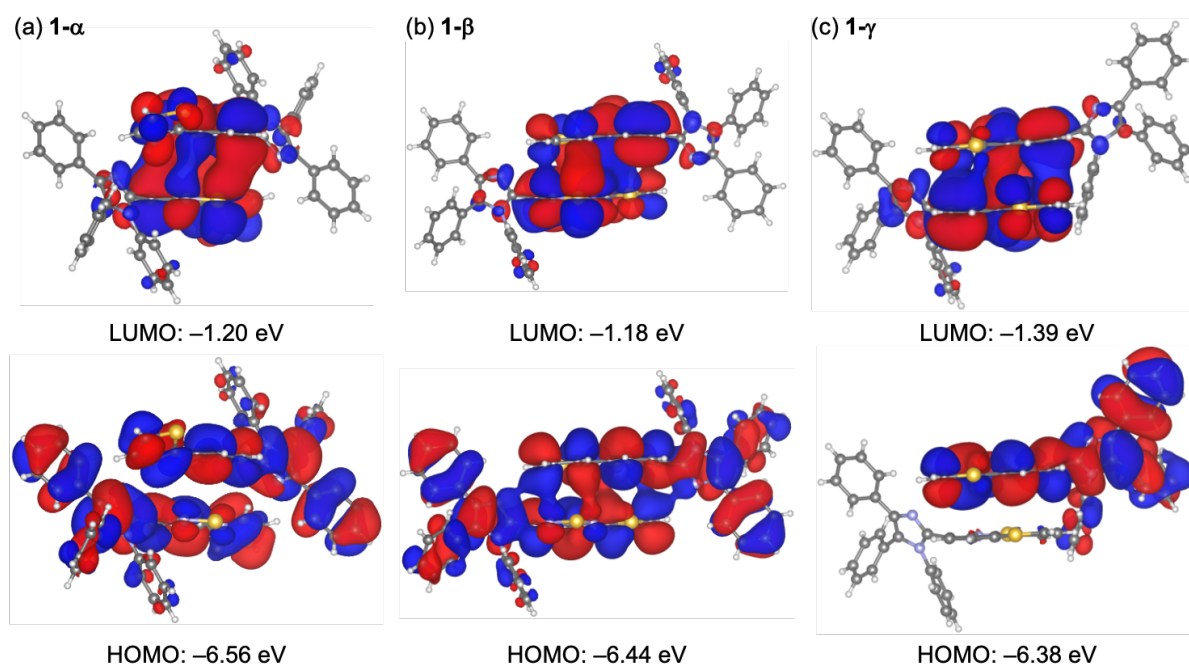


Fig. S8 HOMO and LUMO of dimer **1** in **1- α** (a), **1- β** (b), and **1- γ** (c) calculated at the CAM-B3LYP/6-31G(d) level. The structures are drawn by VESTA.¹

6. PXRD analysis

The experimental PXRD pattern for the heated samples of **1- β** were in good agreement with the calculated PXRD pattern for the single-crystal X-ray diffraction structures of **1- γ** , indicating that **1- β** changed to **1- γ** upon heating (Fig. S9).

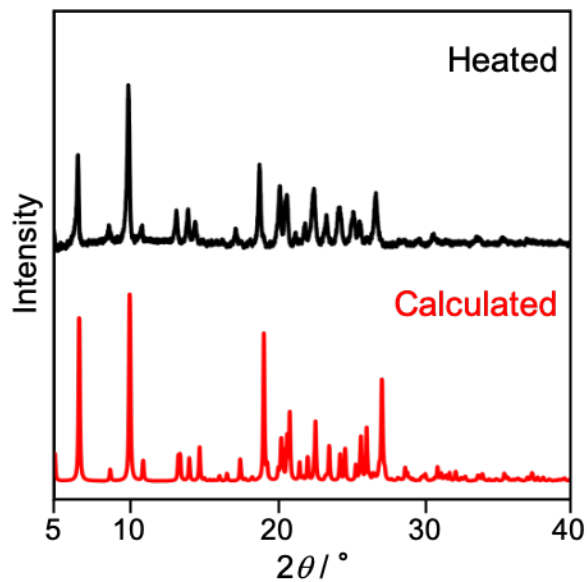
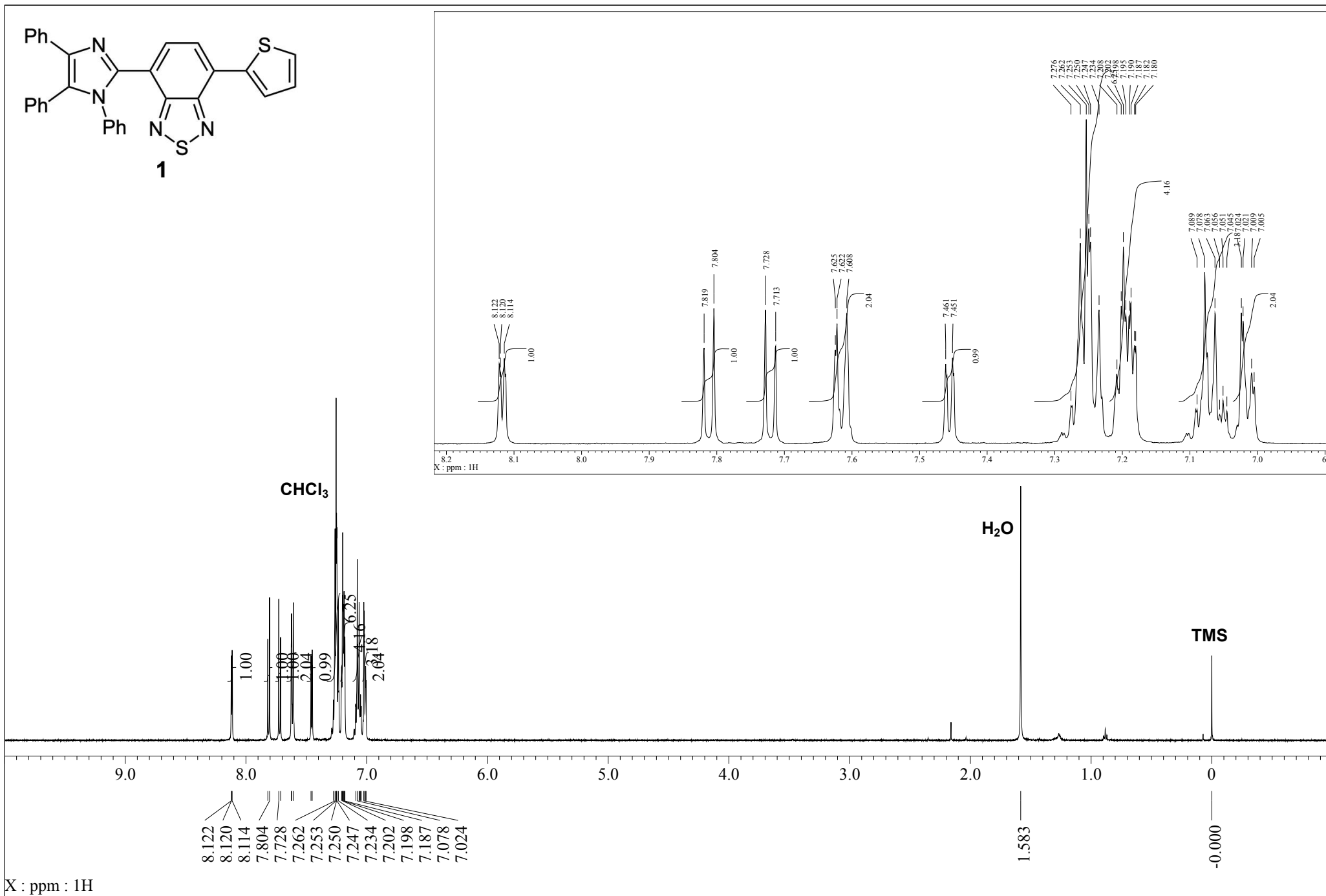


Fig. S9 Experimental PXRD pattern for the heated sample of **1- β** (black line) and calculated PXRD pattern for the single-crystal X-ray diffraction structures of **1- γ** (red line).

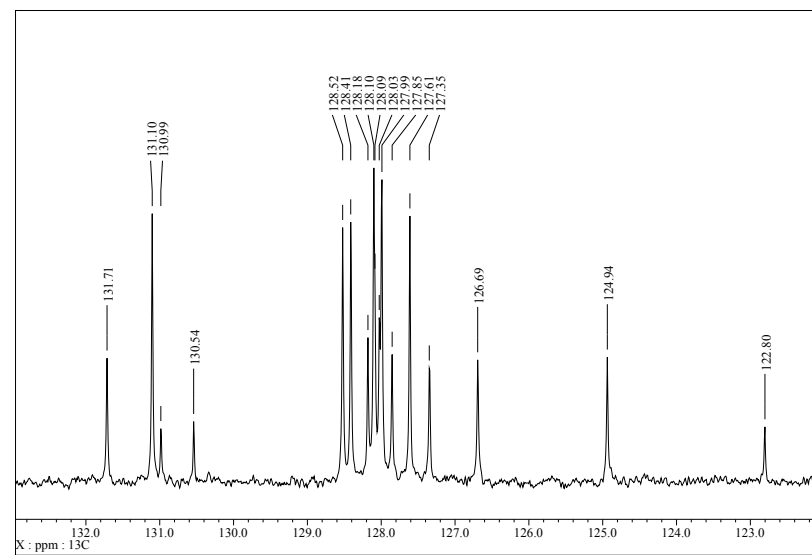
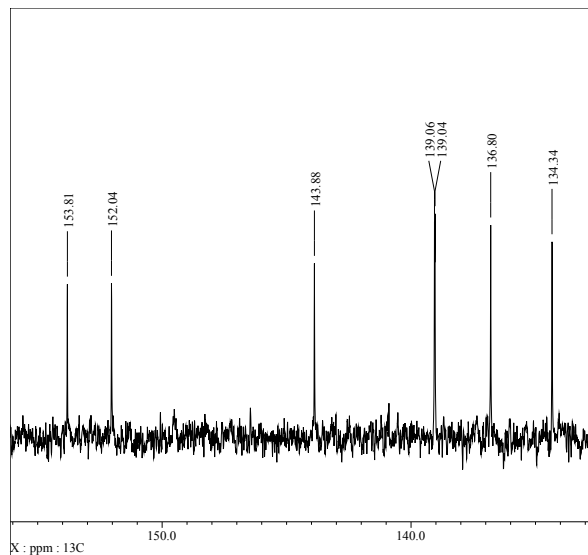
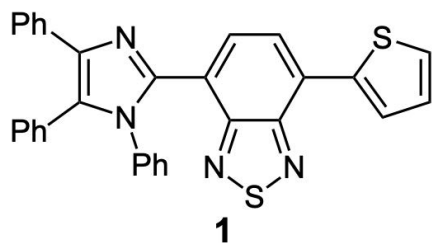
Reference

- 1) K. Momma and F. Izumi, *J. Appl. Crystallogr.*, 2011, **44**, 1272.

¹H NMR spectrum of 1 (500 MHz, in CDCl₃, rt)



¹³C NMR spectrum of 1 (126 MHz, in CDCl₃, rt)



CDCl₃

